DEVELOPMENT OF VOID FRACTION MEASUREMENT SENSOR

Submitted in partial fulfilment of the requirements
of the degree of
Bachelors in Mechanical Engineering

By

Mr. Ashish Rasquinha
Mr. Nichol Rodrigues
Mr. Stanley Vijay

Under the Guidance of
Prof. (Dr.) N.M. Rao
Prof. Deepika Gupta

Department of Mechanical Engineering
Don Bosco Institute of Technology
University of Mumbai
2018 - 2019

Prof. (Dr.) N. M. Rao

Prof. Deepika Gupta

Mr. Ashish Rasquinha

Mr. Nichol Rodrigues

Mr. Stanley Vijay

CERTIFICATE

This is to certify that the project entitled **Development of Void Fraction Measurement Sensor** is a bona fide work of **Mr. Ashish Rasquinha, Mr. Nichol Rodrigues**, and **Mr. Stanley Vijay** submitted to the University of Mumbai in partial fulfilment of the requirement for the award of the degree of Undergraduate in Mechanical Engineering.

20/5/19

Ms. Deepika Gupta
Project Co-Guide
Asst. Professor

20/05/19

Ms. Cleta Pereira
Project Coordinator
Asst. Professor

20/05/19

Dr. N. M. Rao
Project Guide and
Head of Mechanical Engineering
Department

Dr. P. [illegible]inbiar
Principal

PROJECT REPORT

This project report entitled **Development of Void Fraction Measurement Sensor** by **Mr. Ashish Rasquinha, Mr. Nichol Rodrigues, & Mr. Stanley Vijay** is approved for the degree of Bachelor of Mechanical Engineering.

Examiners:

1. Name: Komal Pawar

   Signature: 

2. Name: Dr. N. M. Rao

   Signature: 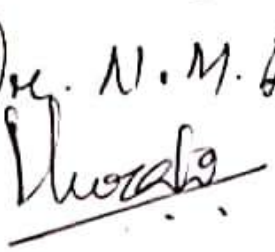

Date: 27.04.2019

Place: Mumbai

Declaration

I declare that this written submission represents my ideas in my own words and where other ideas or words have been included, we have adequately cited and referenced the original sources. I also declare that we have adhered to all principles of academic honesty and integrity. and have not misrepresented or fabricated or falsified any idea/data/fact/source in my submission. I understand that any violation of the above will be cause for disciplinary action by the Institute and can also evoke penal action from the sources which have thus not been properly cited or from whom proper permission has not been taken when needed.

1. Mr. Ashish Rasquinha Signature: 

2. Mr. Nichol Rodrigues Signature: 

3. Mr. Stanley Vijay Signature: 

Date: 27-04-2019

Place: Mumbai

Abstract

Void fraction measurement devices are generally intrusive; a conductivity probe, for example, requires extraneous effort in installation. Additionally, introducing an obstacle in the flow can disrupt flow, change void fraction characteristics, making intrusive void fraction sensors unreliable, especially for flows at high velocity. On the other hand, non-intrusive void fraction sensors exist, but are not suitable for measuring the void fraction over the entire cross-section.

This paper aims to introduce a method to perform non-intrusive measurement of void fraction across the entire cross-section of a pipe. We make use of lasers emitting visible light of wavelength 650 nm to form a light grid passing through the cross-section of a pipe. Changes in medium in the pipe, due to flow of air, cause the light to deflect; the period for this deflection gives the size of the void, and the location of the laser beam that is deflected gives the position. In this study, we have designed our instrument for two-phase flow using water and air flowing through a transparent acrylic pipe having a diameter of 4in, and validated readings with a conductivity probe, based on an existing design.

Acknowledgements

We would like to thank Don Bosco Institute of Technology, and by extension the University of Mumbai, for providing us the education and skill set required to work on our project.
We would especially like to thank our guides Dr. Rao and Ms. Gupta of the Mechanical Department for their valuable insight about our project, and unfaltering support in helping us perform our tasks. Without their help, we may not have made it thus far. We would also like to thank Professor Yogesh Gholap of the Electronics and Telecommunications Branch for his contribution in making the processing circuit for our conductivity probe, and for his guidance on the electricals of our project; and Mr. Norman Abreo for helping us in 3-D printing the instrument.

Contents

Abstract vi
Acknowledgements vii
List of Figures ix
1. Introduction 1
1.1 Needs of Void Fraction Measurement Sensors 1
1.2 Current Trends in Void Fraction Measurement Sensors 1
1.3 Use of Lasers to Measure Void Fraction 2
2. Review of Literature 3
2.1 Void Fraction and Flow Regimes 3
2.2 Principle of Conductivity Probe and Wire Mesh 3
2.3 Principle of Sensor 4
2.4 Reasoning Behind Using a Laser Grid 6
3. Design and Fabrication 7
3.1 Design and Fabrication of Wire Mesh 7
3.2 Design and Fabrication of Conductivity Probe 8
3.3 Design of Laser Sensor 11
3.3.1 Prototype Design 11
3.3.2 First Iteration of Sensor Design 12
3.3.3 Limitations of Initial Design of Sensor 15
3.3.4 Second Iteration of Sensor Design 16
3.3.5 Design of Electrical Circuit 19
3.3.6 Limitations of Second Design 21
4. Results and Discussions 22
5. Conclusions 24
Appendices 25
Appendix I: Arduino Code for Initial Prototype 25
Appendix II: Calculation of Angles for Alignment of Laser Diodes 26
References 28

List of Figures

2.1	Types of Flow Regimes	3
2.2	NIR-based Measurement Sensor, Wang et al. [7]	4
2.3	Schematic of Measurement Sensor	5
3.1	Wire Mesh Design Model, for 2 in diameter	7
3.2	CAD Model of Conductivity Probe	8
3.3	Labelled Schematic of Conductivity Probe	8
3.4	Traversing Mechanism with Conductivity Probe	9
3.5	Wall Flashed Electrode (Brass Foil)	9
3.6	Conductivity Probe	10
3.7	Circuit Diagram for Arduino Prototype	12
3.8	Fully Assembled Laser Clamp, First Design	12
3.9	Side View of Clamp, Right Grid	13
3.10	Side View of Clamp, Front Grid	13
3.11	Top Sectional View of Top Layer of Clamp	14
3.12	Dovetail on Clamp	15
3.13	Hinge Assembly, with dovetail slots	15
3.14	Side View of Clamp, Right Grid	17
3.15	Side View of Clamp, Front Grid	17
3.16	Top Sectional View of Top Layer of Clamp, New Design	17
3.17	Circuit Diagram for Power Supply to Laser Diodes	19
3.18	Circuit for the output of the LDRs to the Data Logger	20
4.1	The Voltage Outputs by the LDRs in terms of Integers on a Serial Board	22
6.1	Calculations of Angles of Orientation for Laser Diodes	26

Chapter 1
Introduction

1.1 Needs of Void Fraction Measurement Sensors

Gas-liquid two-phase flow is a very crucial component in small-channel systems, such as chemical reactors and heat exchangers, and in medium-sized channels, as those used in process industries, such as the food and beverage industry, and the pharmaceutical industry. Void fraction is one of the parameters of primary importance in multi-phase flow. It is defined as the fraction of the channel volume that is occupied by the gas phase, or the fraction of the channel cross-sectional area that is occupied by the gas phase. Measuring this is very important from the point of view of other parameters like efficiency of heat and mass transfer, and also to gauge the safety of the channel under working conditions.

Void fraction is important in a myriad of fields as listed by Evgenidis and Karapantsios, from petroleum processing and extraction of oil and gas, to scuba-diving, subway construction, open-heart surgery, and even space travel [1]. There are many reasons void fraction would need to be measured: one is to monitor anomalies and thus detect any faults in, or damage sustained by a piping system. In fact, this is the principle behind water immersion leak detection, a primitive method of leak detection in pipes. Another is to monitor the efficiency of transfer in a two-phase flow in a pipe.

However, as times go by, the needs of channels in process industries change, as parameters like the velocity of the fluid and the dimensions of the channel, change. This renders the conventional measurement methods unable to satisfy the requirements of industries in the modern age.

1.2 Current Trends in Void Fraction Measurement Sensors

There are numerous ways in which void fraction can be measured. Currently, the onus is on use of non-intrusive methods of void fraction measurement. Some have made use of high-speed imaging in their studies [2] [3], while have used laser diodes and light attenuation [4] [5].

Older void fraction sensors, conductivity probes and wire mesh setups for example, are generally intrusive in nature, i.e. a part needs to be in contact with the flow. This becomes inconvenient, as such an arrangement would need complex and time-consuming installation, and regular, meticulous maintenance. As an example, a conductivity probe would have to be fitted to a traversing mechanism, manufacturing which would be cumbersome as all the necessary tolerances would need to be close; and then the setup would have to be mounted on a pipe, which needs a hole drilled in to let the probe into the two-phase flow. Likewise, a wire mesh would have to be installed similarly to a flange in between two pipes.

Also, the intrusion of a foreign object into the flow could have dire consequences on the flow and the system in which the flow is occurring; it can cause problems like exposure, erosion

of probe, corrosion, and flow disruption, which can hamper accurate description of characteristics in the system [6].
Thus, the need of a new-age sensor, especially in process industries, is that it would have to be non-intrusive.

1.3 Use of Lasers to Measure Void Fraction

Li et al. mention, that due to their accuracy and their short response time, optical void fraction measurement methods are very attractive for accurate measurement [5]. Currently, optical tomography and high-speed cameras are the most accurate techniques of this kind. However, they are not used in industries, as they are very costly and difficult to set up, for example, the lighting requires to be adequate, with halogen light sources and a dark curtain behind for example, as shown by Dragomirescu et al [2]; a setup that is not feasible in a factory.

On the other hand, a lot of prior research has been done in using light sources to detect void fraction, both in the visible spectrum [5] and out [7]. A recurring theme is the use of light attenuation factors, in which the intensity of the light beam is changed depending on the bubbles passing through the section. This would work well for setups with highly sensitive photodiodes. However, diodes of such sensitivity may be expensive, compared to light-dependent transducers (LDRs), and may be prone to error in factory environments if not properly handled.

Another approach could be the use of refractive index and change of such due to flow of bubbles in a pipe, as demonstrated by Malmstrom et al [8]. Thus, the objective of this study is to develop an instrument to accurately measure void fraction non-intrusively, and to corroborate any such measurements made by this device with a veritable source: a conductivity probe, whose development is in-house.

Chapter 2
Review of Literature

2.1 Void Fraction and Flow Regimes

There are various flow regimes, depending on the orientation of the pipe. If horizontally oriented, gravity becomes a dominating force in the flow. This governs the direction in which bubbles will rise, and the side of the pipe which water and heavier particles, if any, will stick to. Besides gravity, there are many other factors determining void fraction: velocity of flow, quality of sealing, obstructions, etc. Some examples of flow regimes are given in the figure below. Each flow regime is easily identified by the void fraction, and the location of voids in the pipe.

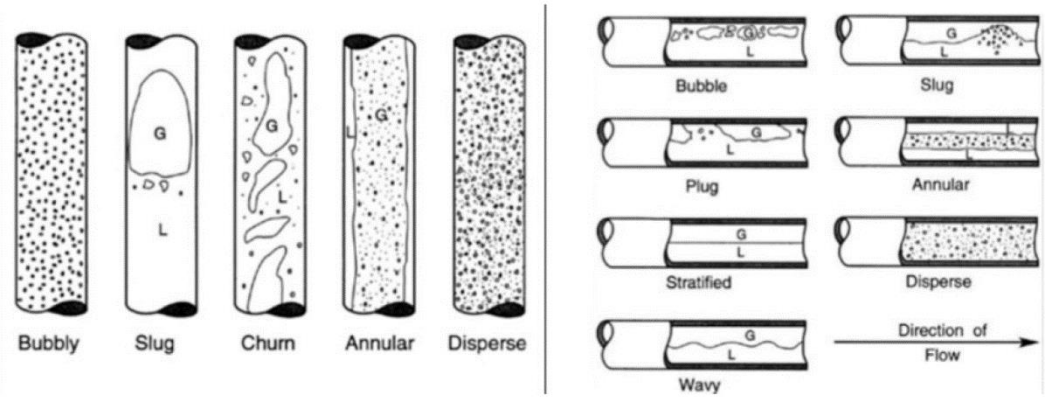

Figure 2.1: Types of Flow Regimes

2.2 Principle of Conductivity Probe and Wire Mesh

A conductivity probe consists of simply one conductive needle, and a conductive foil surrounding it, which is applied on the inside of the pipe where testing is done. The principle of the conductivity probe is simple; if a void comes in between the needle and the foil, a change in resistance occurs. This change in resistance is recorded as the presence of a void.
The working of the wire mesh is similar, except that instead of using a needle, it uses a steel mesh. The mesh would be naked at the points of intersection, but insulated everywhere else. This would have the effect of having several needles in the pipe, to test the flow regimes. This would be effective in observing the characteristics of void fraction throughout the cross-section of the pipe. However, these sensors are still intrusive sensors; they have their set of disadvantages on the flow on the flow system [6].

2.3 Principle of Sensor

The pipe to be tested is oriented vertically, and the direction of flow is upwards. Light is fired through the tube with flowing water, such that it falls on a receptor which is diametrically opposite the source of light. This light passes through effectively 2 media, including that of the pipe (glass or acrylic). If a void is formed due to passage of air, it would flow upwards, in the direction of water flow. If the void passes through a beam of light, that light beam would effectively pass through 3 media: the pipe, water, and the air in the void. Due to this, and the fact that the surface of the void would generally be inclined to the light, the laser would be deflected off of the receptor. This absence of light on the receptor would be detected, and this is the factor that would tell whether or not a void has passed.

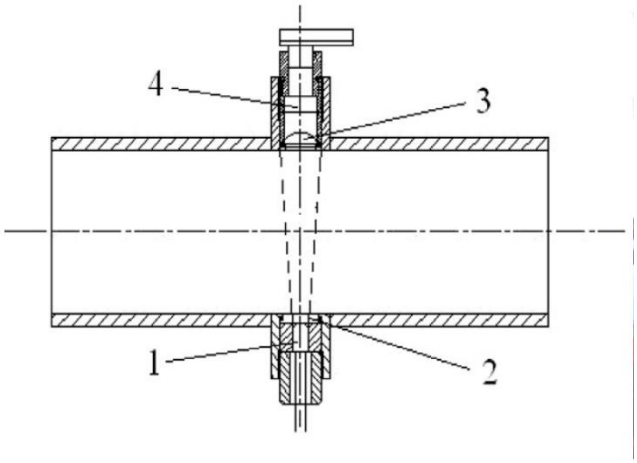

Figure 2.2: NIR-based Measurement Sensor, Wang et al. [7]
Labels: 1- GaAs NIR LED, 2 – Quartz glass, 3 – Quartz lens, 4 – Photoelectric integrated circuit

The trend in light-based void fraction sensors, as exhibited in previously developed sensors [7], and in other studies, is that they are generally single-point; they only pass through a point or line in one plane only, generally lying in the plane of the cross-section. Due to this, many voids in the pipe may be missed, as the light cannot cover the entire cross-section. Only the voids formed in the region that the light would pass through would be detected.

Another laser-based sensor has been described [5], to measure the void fraction in a channel with a diameter under 5 mm, in which a laser beam was split into multiple smaller beams, such that they would pass parallel to each other through the tube. While effective, however, this arrangement is only feasible for a small channel diameter, as the conditions do not vary much through the cross-section.

Due to budget and time constraints, and due to lack of availability of such photoreceptors sensitive to small changes in light intensity, we had to use the current laser-LDR setup.

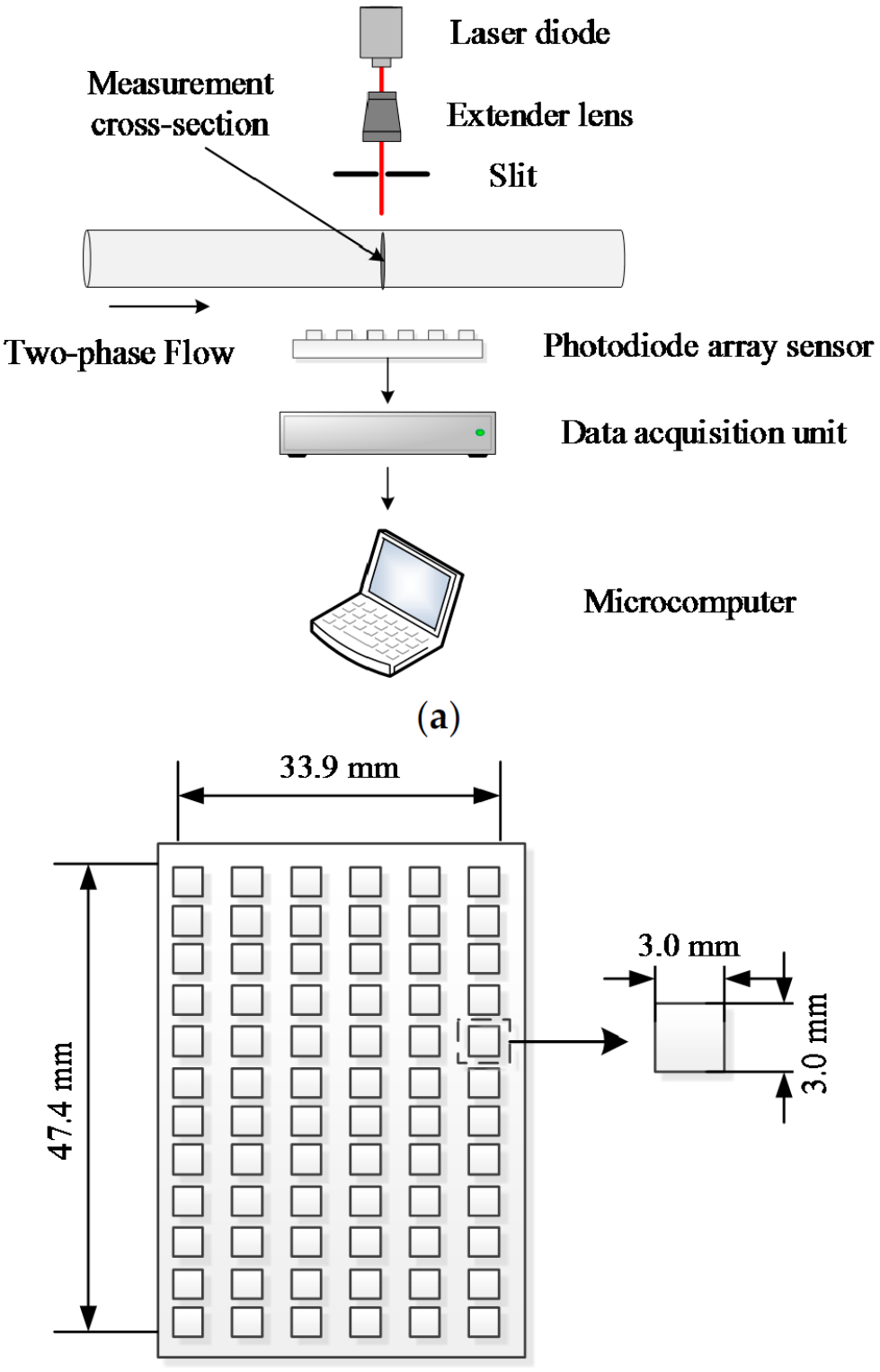

Figure 2.3 (a): Schematic of Measurement Sensor, (b): Photodiode Array, Li et al. [5]

2.4 Reasoning Behind Using a Laser Grid

Upon consideration, we deduced that a laser wall on only one axis would be insufficient, because of the nature of divergence of light. If a void were to come between an emitter (laser diode) and a receiver (LDR), the light beam would get deflected, and the interruption would be recorded by the corresponding receiver. However, if there were multiple voids passing through the same vertical section of the pipe, the void closest to the emitter would deflect the beam, leaving the other voids undetected. This could be solved by adding a second wall of lasers, which is perpendicular to the first grid, but in the same plane, or a plane parallel to the first grid, forming an effective laser grid, to measure the void fraction in a given cross-section.

The benefits of such a setup is that it would be able not just to notify when a void has passed through, but also the position and size of any given void, and the number of voids passing through with reasonable accuracy. Once one such unit is made, multiple units can be used concurrently, in a series, to give the void fraction characteristics in a certain section of the piping network. These can also be used to give the velocity of any void flowing through the section under scrutiny. This laser grid would look similar to a wire mesh setup, as has been used before.

Chapter 3
Design and Fabrication

3.1 Design and Fabrication of Wire Mesh

The wire mesh was designed for a 2in diameter pipe. The flange was provided by college, using the dimensions of which we designed the wire mesh, finding the holes that needed to be drilled to weave the wire through. These holes would be 1.5 mm in diameter, so that the obstruction provided by the resulting mesh would be minimized. There would, however, be some obstruction, as this is still an intrusive sensor.
After making the flange, a steel wire of adequate size is used to make the mesh. We selected a 1mm diameter wire based on availability and the size of drill that was used to make the holes in the flange.

Figure 3.1: Wire Mesh Design Model, for 2 in diameter

The wire mesh was made from an acrylic flange and a steel wire. Small 1mm holes were drilled along the periphery of the 2in hole at the center of the flange, through which the wire was woven to form a mesh, much like a tennis or badminton racquet. This wire mesh setup would be connected to one lead of a processing circuit, and the other would be connected to a foil on the inside of the pipe, where the testing is being done.

3.2 Design and Fabrication of Conductivity Probe

A CAD model of a conductivity probe was also made. This would be used to verify the results of the laser sensor and the wire mesh. The conductivity probe needle is movable, from the centre to the wall. It is assumed that the voids would not vary much azimuthally, i.e. in that cross-section.

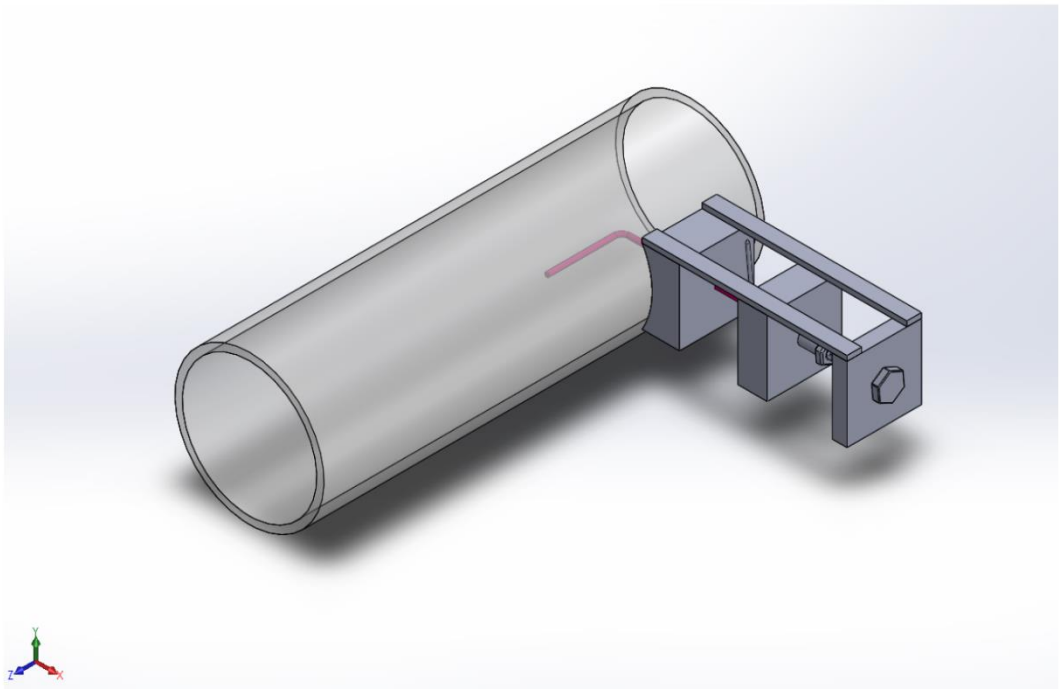

Figure 3.2: CAD Model of Conductivity Probe

The conductivity probe consists of three major parts: the traversing mechanism, the probe, and the foil.

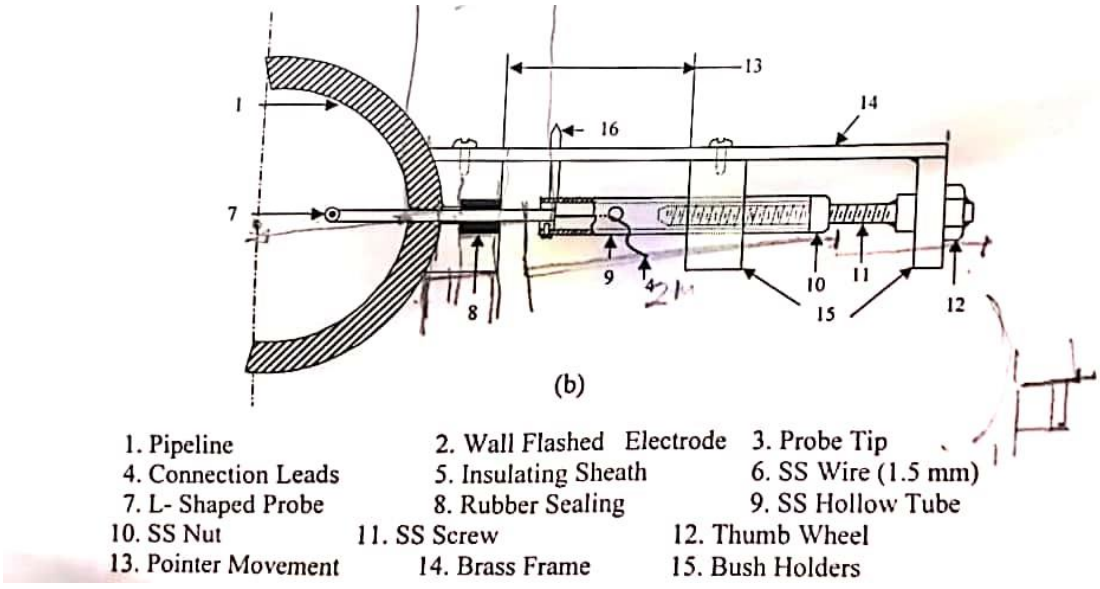

Figure 3.3: Labelled Schematic of Conductivity Probe

Traversing Mechanism: To be able to measure the void fraction characteristics of two-phase flow at multiple places in the cross-section of the pipe, the probe must be able to move. Hence, there is a traversing mechanism, that provides radial movement of the probe. The mechanism consists of parts 8-15 in Fig. 6, and is mounted on the pipe by sticking the block containing the rubber seating using an adhesive. The block has a concave cut of 4 in diameter, to fit well on the pipe.

The pitch of the stainless-steel screw (11) is very small to allow for very precise movements of the probe in the pipe. The stainless-steel nut (10) connects to the stainless-steel tube (9), which houses the connection lead for the probe (4), and the probe itself (7). The tube and the screw are mounted and constrained by the bush holders (15), such that the screw can only be rotated, it cannot translate. The screw is turned with the thumb wheel (12).

Conversely, the tube can only translate; the pointer (16) constrains the tube such that it cannot rotate. Thus, turning the thumb wheel produces a translatory motion, which gets transferred to the probe. The entire mechanism is held together by a steel frame (14).

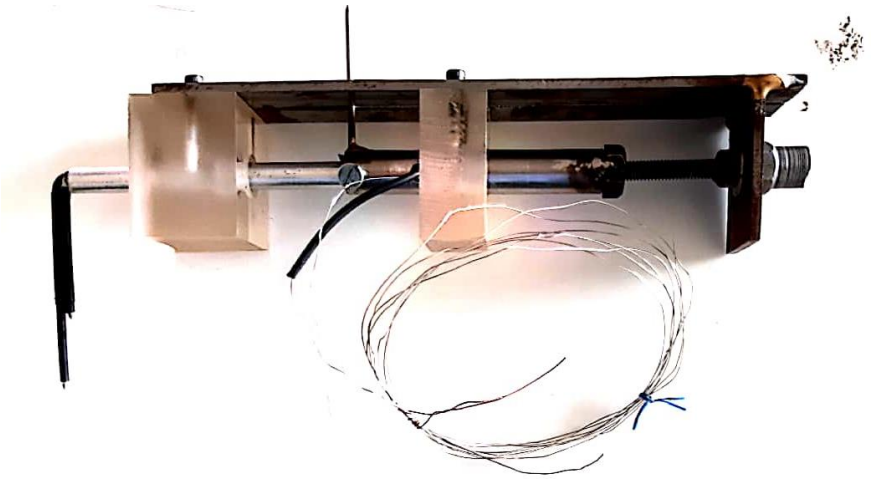

Figure 3.4: Traversing Mechanism with Conductivity Probe

Wall Flashed Electrode (Brass Foil): This brass foil is pasted on the inside of the pipe, and is connected to a lead using solder to the processing circuit. This acts as a negative terminal for the processing circuit. It is between this and the probe that the resistance of the flowing fluids is measured, and the void fraction is found out for that section.

Figure 3.5: Wall Flashed Electrode (Brass Foil)

Conductivity Probe: The conductivity probe is just a pointer that is inserted into the pipe through a hole on the wall of the pipe. The probe itself is made of a stainless-steel L-rod, which is sharpened at the tip of the shorter limb of the L. It is then surrounded by a rubber sheath, to insulate the probe everywhere except at the sharpened tip. This is to make the probe detecting area as small as possible, for accurate results. The probe is oriented such that the

The probe is connected to the traversing mechanism via the stainless-steel tube, and moved between the center of the pipe, to the wall. Thus, it is able to measure the resistance between itself and the brass foil.

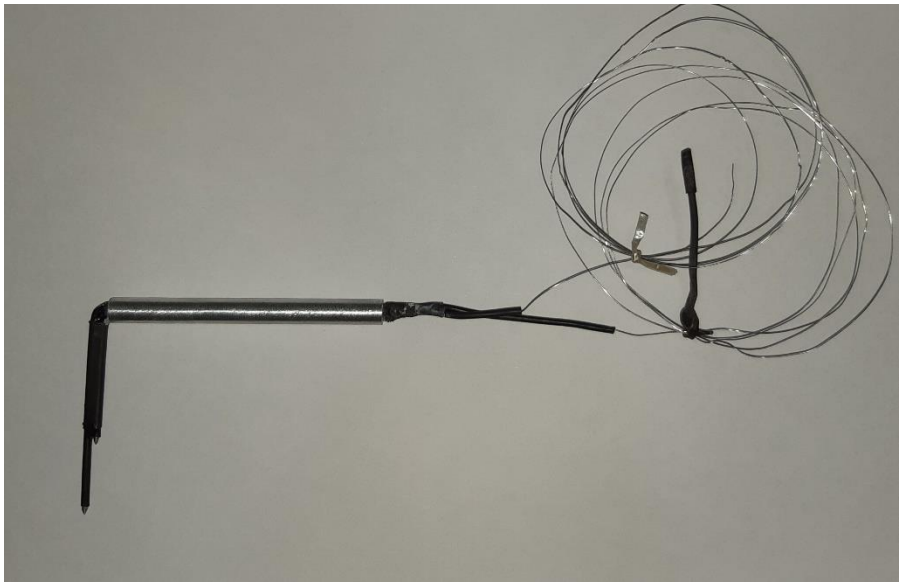

Figure 3.6: Conductivity Probe

A design change that was made to the conductivity probe to increase its utility is to take two probes as described earlier, stack them on top of each other such that there is a distance between the two tips in the axial direction, and insert them into the pipe simultaneously. This enables us to take another measurement pertaining to the void fraction of the two-phase flow system: the velocity of a given void. How this works is simple: the distance between the points is constant throughout the period of usage, it will not change in the pipe when two-phase flow is active. Due to this distance, there will be some time interval between the two points of measurement; when the void passes through each cross-section. Using a stopwatch (or for an even more sophisticated method, a data logger), this time interval can be measured, and given the formula for speed, the speed of the void can be calculated. If the direction of void flow is known, we now know the void velocity.

3.3 Design of Laser Sensor

The laser measuring principle is the central idea of this study, and the design must be adequate to demonstrate the working of this principle.

3.3.1 Prototype Design

We fashioned our first prototype using an Arduino Duemilanove board, one laser diode, one photoreceptor, one LED and jumper wires. The laser diodes used are Circuit Systems M417, 3 V, 5 mW diodes, outputting light of 650 nm wavelength. The photoresistors used for receiving light are Component7 B00C743131, with a detecting surface area of about 3 mm × 3 mm. This setup was design not for a piping network, but for a small-scale testing setup, consisting of a soda-lime-silica water glass, and a plastic straw, through which one would blow through from the top, generating bubbles in the water, which would be the void fraction for which testing would occur.

The problem with this is, the laser and the photoresistor would have to be held in place by hand, making testing very inconvenient. Also, due to constraints in our initial testing setup, bubbles would only be formed on one side of the glass, and the laser would often miss its mark, unless very painstakingly positioned.

In the second iteration of making the prototype, two lasers were used (due to lack of jumper wires, only two), and the Arduino code was altered such that if either laser was blocked, i.e. if either photoreceptor was not receiving light, the board would detect the disturbance in the signal & so through the serial monitor. We also used pieces of mount board to make the holders for the lasers and the photoresistors, which can be pasted to the glass, making testing more convenient than before. (For the code for the prototype, see Appendix I).

This Arduino-based prototype was sufficient for initial testing, and was a broadly simplified edition of the final design. Based on this, a laser sensor making use of the principle was developed. Since the design was too complicated to accurately manufacture just by machining, rapid prototyping through 3-D printing was used. 3-D printing was done in college initially, since it could not be worked the whole day, the printing time had to be reduced drastically. Due to this, many other considerations had to be taken.

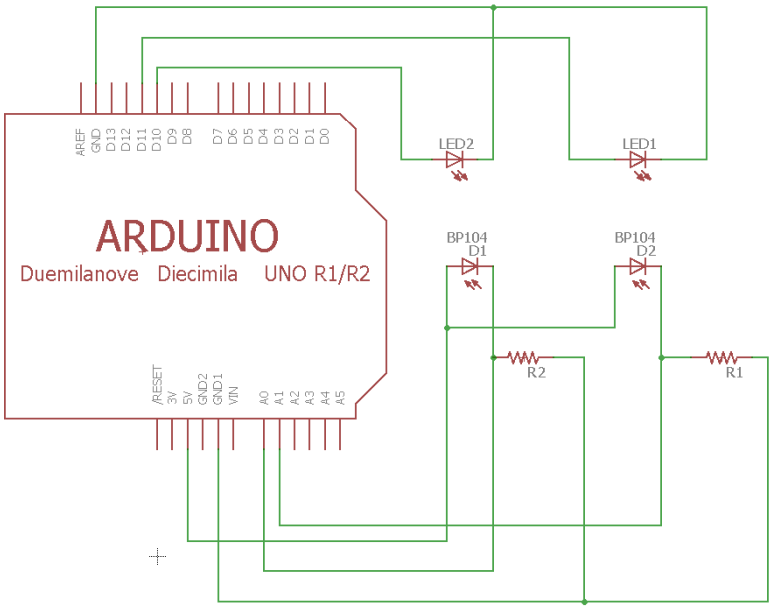

Figure 3.7: Circuit Diagram for Arduino Prototype

3.3.2 First Iteration of Sensor Design

The first laser sensor had a design much more involved than the Arduino prototype, but was still simple. Many more laser diodes were used compared to the prototype. The sensor was designed for a 4 in diameter acrylic pipe, with a thickness of about 3 mm.

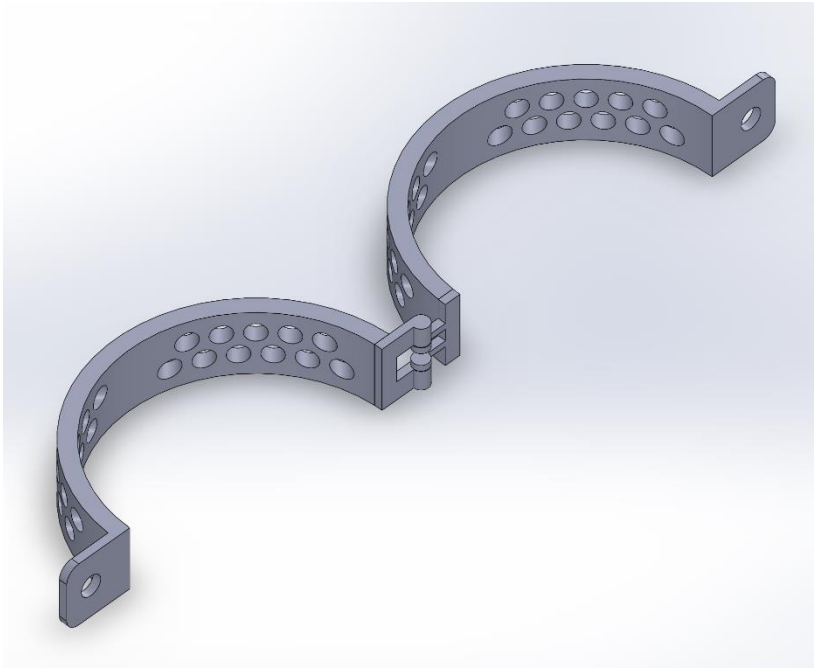

Figure 3.8: Fully Assembled Laser Clamp, First Design

An initial complication was that due to the laser diodes being 6mm in diameter, making a grid small enough to pick up even the smallest of voids would be impossible with our resources. That would only be possible if an arrangement using a beam extender and a beam

splitter could be made, to create a wall of lasers, like the one demonstrated by Li et al [5]. Size and material considerations in 3-D printing would also be needed. Thus, would not allow for a singular laser grid smaller than 10 mm × 10 mm. To work around this, we made use of a second layer of lasers, such that each laser on the bottom layer is equidistant from the lasers on top, i.e. in between two lasers, but also at 10 mm distance from each of them, forming cells of equilateral triangles. This is done to increase the resolution of the effective grid, making it 5 mm × 5mm in size, greatly increasing accuracy. A side-effect of this design was that the principle of measuring void velocity can also be seen here, as there is some distance between the layers of lasers. The time interval could be measured easily with a data logger.

There are two layers of grids in the sensor: both 6 lasers × 5 lasers in dimensions, with the lower grid oriented 90° to the upper one.

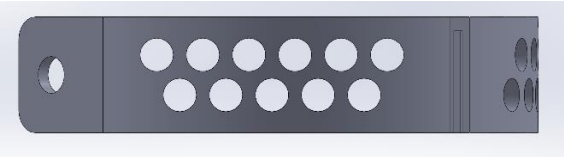

Figure 3.9: Side View of Clamp, Right Grid

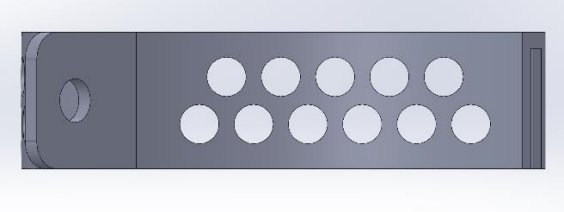

Figure 3.10: Side View of Clamp, Front Grid

This is done to make sure that both grids have equal probability of detecting the presence of a void, to keep readings uniform; if a 6 × 6 laser grid was to be used, it would detect more voids than the lower 5 × 5 grid. This means that there is a total of 22 lasers in the sensor. This size was chosen to cover as much of the area of the cross-section without having to forsake structural strength of the instrument; due to positioning of lasers, the material to hold them may decrease. For this, there were holes made in the circular parts of the clamps of 7.2mm in diameter. This size was chosen to account for shrinkage and warping of the material while printing; about 0.6 mm on each side. This was found to be too much. The thickness of the clamp was 6 mm thick, to allow the diodes to sit in without having to provide supports.

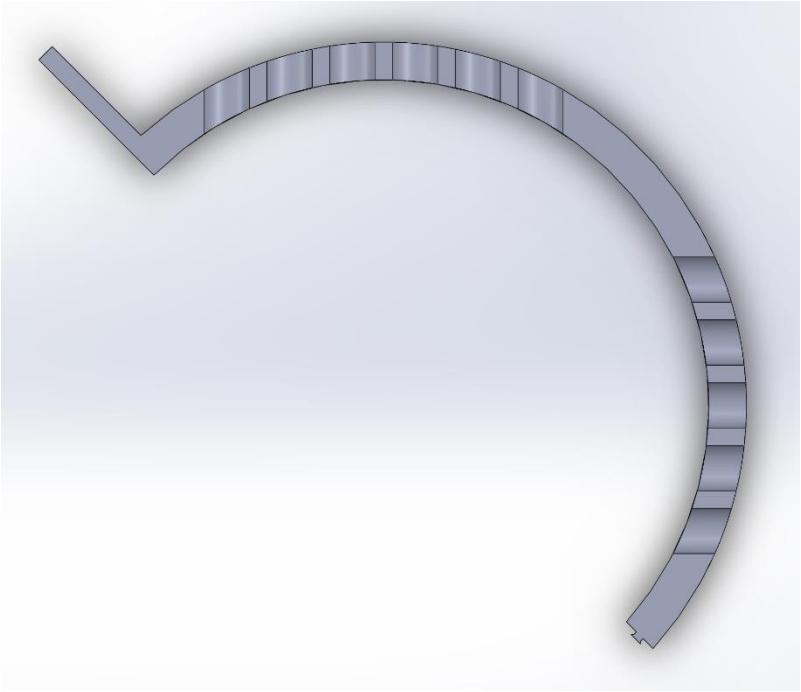

Figure 3.11: Top Sectional View of Top Layer of Clamp

The position and size of the holes for the LDRs was similar to that of the laser diodes, except that they would be mirrored about the diameter; they would be exactly opposite their corresponding diodes, such that the lasers would fall on the diodes directly after putting the sensor on the pipe. Unfortunately, this was not the case, as the effect of refraction of the light beams due to water in the pipe was erroneously neglected in the original design. Nevertheless, this was observed only after printing was done.

The clamp portion of the laser sensor was 3-D printed using PLA material, which is sufficiently strong to hold the weight of 22 laser diodes and 22 LDRs. The 3-D printing was done in college, but due to some errors in design and in printing, the sizes of the holes were bigger than intended. To hold the lasers to the 3-D printed clamp, paper tape was used to increase the diameter, so that the space could be occupied. The same was done for the LDRs.

Another consideration while 3-D printing was that of overhanging ledges, which would sag or collapse if allowed to print. However, to make the hinges in the clamp, overhang was unavoidable in the current orientation, which could not be changed. A solution to this was to print the hinges separately, in a horizontal orientation, to prevent sagging; and to use principles of joinery in woodwork: joining the hinges to the main circular part of the clamp by using a dovetail joint, leaving about 0.3 mm tolerance. Due to speedy printing, however, this was seen to be not enough, so it was increased to 0.6 mm.

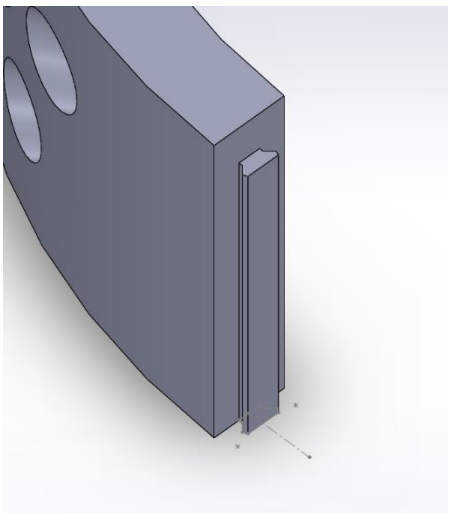

Figure 3.12: Dovetail on Clamp

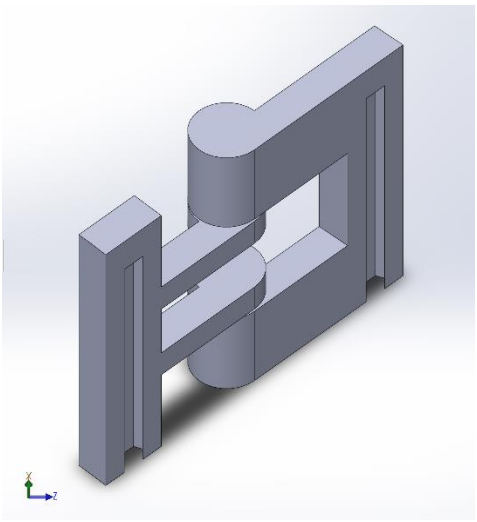

Figure 3.13: Hinge Assembly, with dovetail slots

3.3.3 Limitations of Initial Design of Sensor

Due to water passing through the pipe, the rays of light would be refracted a significant amount, like a convex lens converging the light beams. This was undesirable, as now the light beams were not falling on the LDRs, but were out of place entirely. Moreover, due to using paper tape to hold the lasers in place, between the diode body and the wall of the holes, the laser rays were off the mark; they were not in the same lines anyway. Also, due to errors in rushed printing, the dovetail joint was improper, so initially adhesive was used to hold it together, but this was still just a makeshift arrangement. To overcome these problems, the design had to be changed from scratch.

3.3.4 Second Iteration of Sensor Design

The second iteration of design used a lot of principles from the first iteration, but sea changes were made to the most important elements of the sensor.

The first problem to overcome was the setting the tolerances for the laser diodes and the dovetail. The tolerances were incorrect; they were too big in some places, and in others, due to speedy printing, parts with smaller tolerances were not fitting at all. Thus, printing was instead done from a third-party, where the tolerances of the printer are tighter and printing time can be as long as needed. Thus, the issues of the tolerances were easily fixed. The diameter of the laser holes was reduced to 6.2 mm, and the tolerance for the dovetail joint was reduced to its original value of 0.3 mm. This was much better compared to the original, as the laser diodes could be press-fitted into the holes, and the two halves of the dovetail very snugly fit into each other, with no play, and sufficiently smooth rotation. Another design change was that instead of using through holes in the clamp, counter-bored holes were used, so that the laser diodes would not slip towards the centre of the pipe.

The second problem, the problem of the refraction of laser beams was trickier to solve. Using a CAD software, the intended path of the laser beams was set as the refracted rays. The refracting surface would be the outside of the pipe. We observed that the acrylic walls do not have much effect on the path of the laser beams. This is because the walls of the pipe are too thin to refract the beam significantly; therefore, the refraction by the acrylic can be neglected.

Now that we know that refraction occurs only due to water, we can calculate the angles which the diodes must be oriented to with respect to the normal at each point of incidence, using Snell's Law of Refraction.

For light passing from air through any medium, incident at point of incidence at angle 'i', and angle of refraction 'r',

$$\frac{\sin i}{\sin r} = \mu$$

Where μ = refractive index of medium = 1.33 for water.

(See Appendix II)

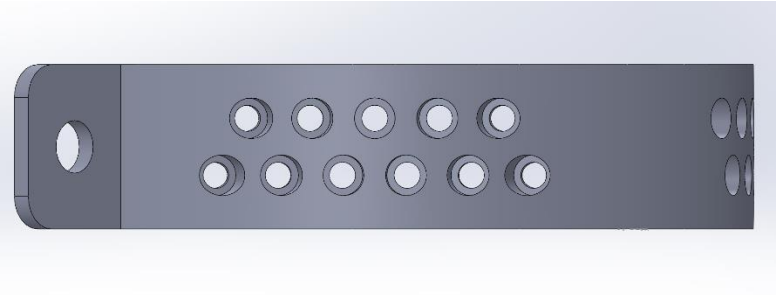

Figure 3.14: Side View of Clamp, Right Grid

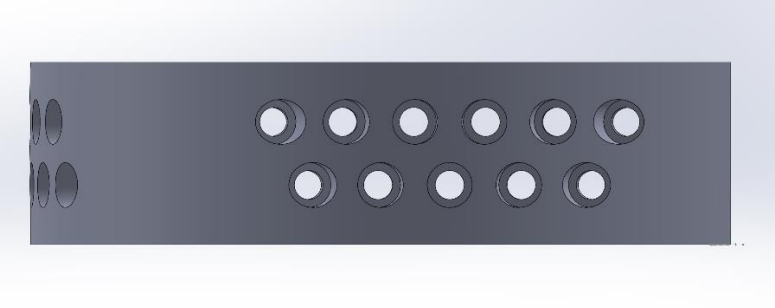

Figure 3.15: Side View of Clamp, Front Grid

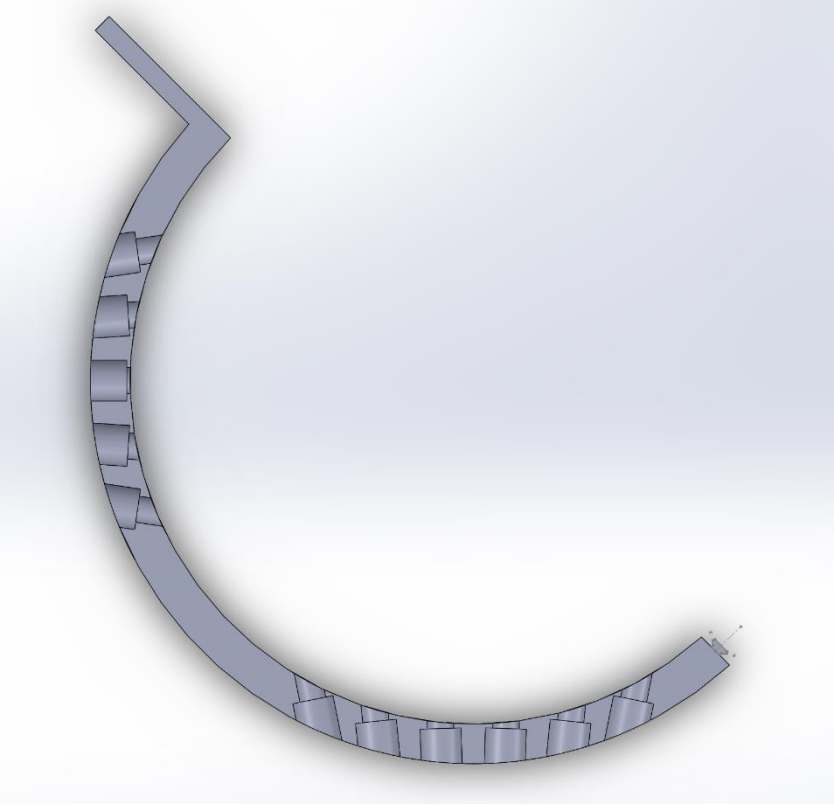

Figure 3.16: Top Sectional View of Top Layer of Clamp, New Design

To the inside of the clamp, strips of rubber gasket material were applied, so that the clamp would not slip off the pipe once clamped onto it.

Another smaller design change was made to the holes holding the LDRs: instead of blank holes holding each LDR, there was a notch made in each position, not extending through the wall, but only to half the thickness, and from there two holes of 1 mm diameter were made, one for each lead of the LDR. That way, the LDRs can just be kept in the notch, while the leads can be removed through the holes, and connected to the data logger and to the circuit through wires.

3.3.5 Design of Electrical Circuit

There are essentially 2 circuits for this laser sensor: the circuit for powering the laser sensors, and the circuit for powering and receiving the output signal from the LDRs. The laser circuit is relatively simple, all the lasers are connected in parallel to each other, and powered by 240 V AC supply. An LED driver is used to convert the output voltage to 12 V DC. The power rating of the laser state that its operating voltage is 5 V, and the minimum power it uses is 5 mW. Thus, the minimum current each diode needs to work is:

$$I = \frac{P}{V} = \frac{5 \times 10^{-3}}{5} = 1\ mA$$

Since the rated voltage is 5 V, and the supply voltage is 12 V, the voltage across the resistor should be 12 – 5 = 7 V, to prevent the lasers from overloading.

Total current drawn = I × no. of lasers = 1 × 22 = 22 mA

Therefore, maximum value of resistor needed to be put before lasers

$$R = \frac{V}{I} = \frac{7}{22 \times 10^{-3}} = 318.18\ \Omega$$

If a resistor of value 330 Ω is used, the value of current flowing through each laser,

$$I_{laser} = {}^{V}\!/_{R}\,/_{no.of\ lasers} = {}^{7}\!/_{330}\,/_{22} = 9.6418 \times 10^{-4}\ A = 0.96\ mA$$

Upon experimentation, it is seen that this is a sufficient current value to give the desired brightness of laser diode, without gradually losing its brightness.

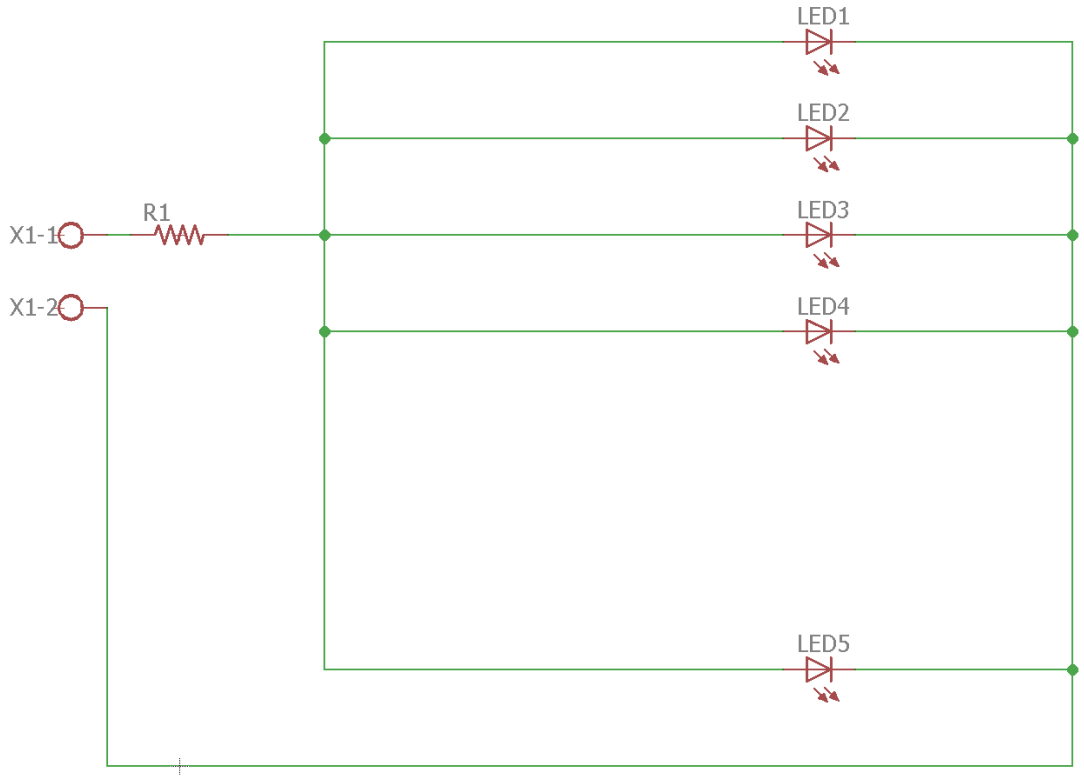

Figure 3.17: Circuit Diagram for Power Supply to Laser Diodes

The second part of the circuit is the LDR circuit. For the LDR to work, it needs to be connected to a 5 V DC supply, like a normal resistor. The resistance between the neutral terminal of the LDR and ground is taken as 100 kΩ. This value was taken on the advice of an advising teacher from our EXTC department. The output of the resistor is connected to a separate lead that is connected to the data logger. The data logger picks up the signal in terms of voltage fluctuation, that depends on the concentration of light falling on it. When no light is falling on an LDR, the output voltage is in the order of 0.1 V, while when the light is falling on the LDR, the output is closer to 5.0 V.

This circuit was made on a solder prototype board, and the output wires used are jumper wires.

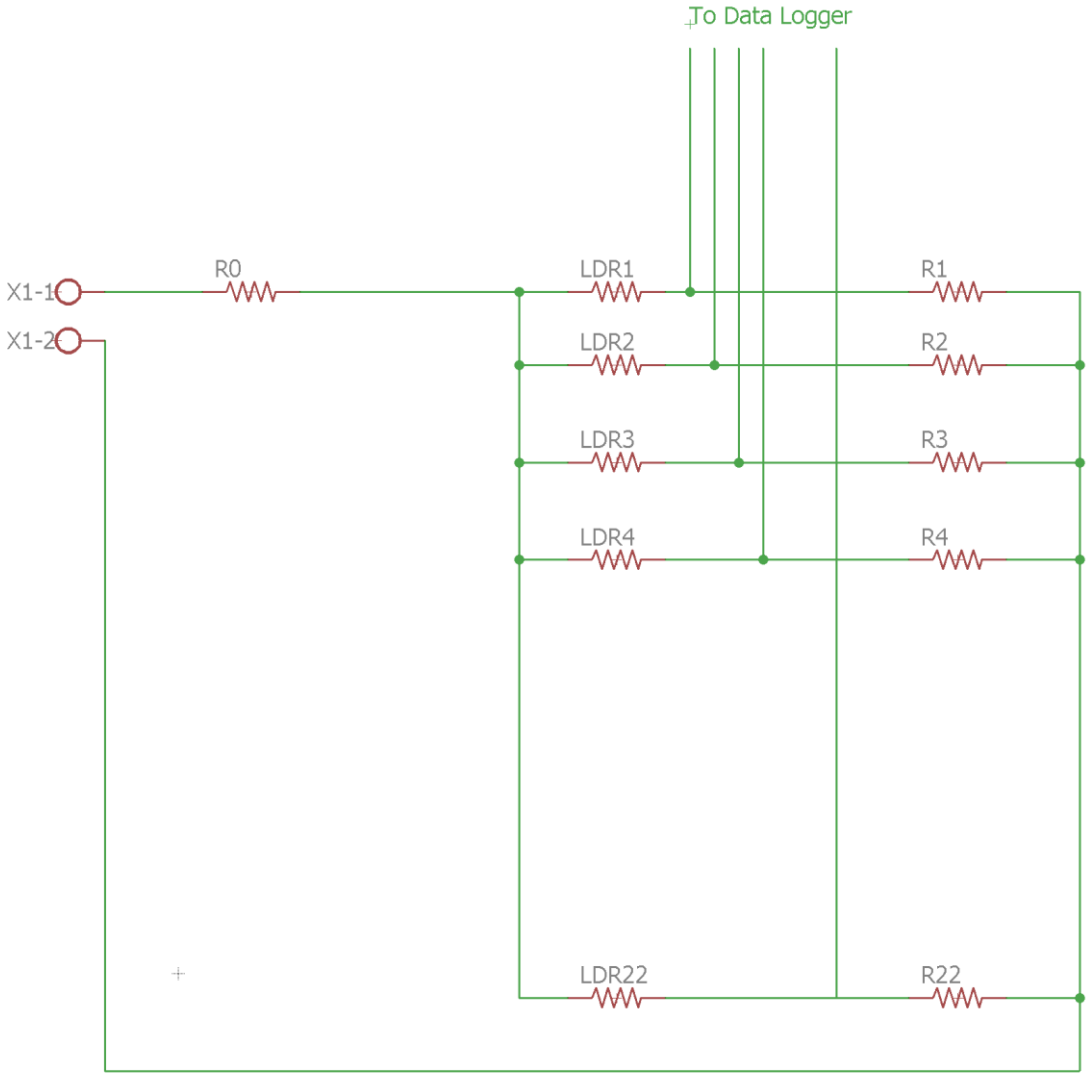

Figure 3.18: Circuit for the output of the LDRs to the Data Logger

3.3.6 Limitations of Second Design

Due to some imperfections in the 3-D printing that were unavoidable with the technology that was available at hand, the lasers still face some uncertainty in their position, and the laser points are still misaligned with each other in the same plane. However, the considerations for refraction were proper, and instead of converging to a central point, the light beams are staying mostly parallel inside the pipe. Unfortunately, most of the lasers are still not falling on the LDRs, meaning that there would be no way to reliably check whether or not the light beam is getting deflected.

Chapter 4
Results and Discussions

The principle of the refraction of laser beams in water is sound, as shown by Malmstrom et al [8], and has been observed in the initial prototype demonstrated with the Arduino, and a small-scale test rig with a glass, straws, and paper. The program (see Appendix I) sends the signal obtained by the LDR in terms of voltage, and converts that voltage into an integer, meaning that if that integer is above a certain value, it could be deduced that the light is on the LDR, and if it is below that, the light is not reaching the LDR.

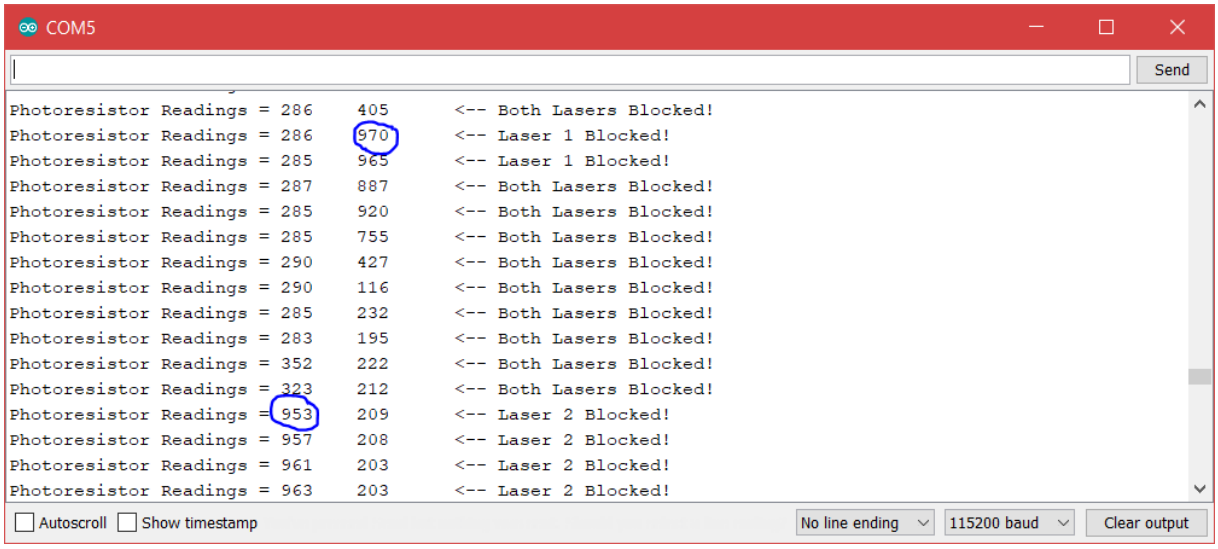

Figure 4.1: The Voltage Outputs by the LDRs in terms of Integers on a Serial Board

In the case of this setup, given the strength of the laser beam during testing, this number was set to 950. Through this, we can see that when the light falls on the LDR, the output is generally above 950, while in the absence of laser light falling on it, the output generally drops down to a maximum of 350.

It should be stated that this lower number depends on the presence of ambient light. It may be higher for brighter rooms, and may dip lower than this value for a dimly lit room. But, as long as the ambient light is not brighter than the laser itself, this would work well. This makes this setup ideal for moderately illuminated industry workspaces.

Another consideration that needs to be taken, while using this clamp, is that transparent acrylic tubes would have to be installed at certain areas in the piping network for this clamp to work, as visible light cannot pass through mild steel. This would still, be easier than say, drilling a hole into a pipe and risking leakages, only to get readings that may be subject to change.

Unfortunately, we were not able to test the full clamp on a piping network, as due to the flaws in the most recent design, the laser grid could not be made reliably. Thus, the testing of the clamp in working condition remains to be seen.

The testing setup is ready and reliable, however; it is a multi-phase flow system developed with the intention of studying multi-phase flow. It contains a pump, to pump water up a maximum height of 3 m, and a sparger to mix air with the water. The tank has a maximum capacity of 1440 liters. The setup can mix water at different pressure drops, and can accordingly give various kinds of void fractions, from bubbly, dispersed, to slug flows and annular flows. These flows are only for the vertical flow regimes, however.

The data logger is also ready: a Hioki data logger with 30 data channels, which can be upgraded to 120 maximum channels. The logger can pick up signals in terms of voltage, and can display them in a voltage vs. time graph. Thus, when this last wrinkle is smoothed out, and the sensor is finally complete, it would be able to give the void position, size, number, and velocity.

Chapter 5
Conclusions

The principle based on which the laser-based void fraction measurement technique has been demonstrated and recreated in the form of prototype design. This principle can be used to detect and measure the presence of void fractions in different kinds of flow regimes in vertical flow.

This sensor is just one unit, to check the void fraction characteristics for just one cross-section; but many of these units can be consecutively assembled such that the void fraction characteristics can be found out for an entire limb of a network.

This approach to void fraction measurement can prove to be a very unique and feasible method to monitor the transfer efficiencies of networks, and to detect flaws in networks early on; without having to deal with the risks and the hassle of using an intrusive sensor.

A lot of expansion can be done to this kind of device, where we used separate laser diodes, beam extenders and beam splitters can be used to create finer grid sizes, or maybe different or mores axes can be used to form grids. A novel technology would be a sensor that has the ability to see through opaque surfaces, like mild steel pipes. However, with current technology, it would not be feasible to implement this practically. For example, visible light cannot pass through mild steel pipes. The kind of light needed to see through metal would be of a much higher frequency (gamma rays, for example); sources of this kind of light are too expensive and dangerous to handle.

Appendices

Appendix I: Arduino Code for Initial Prototype

```
int value1;
int value2;
const int laser1 = 10;
const int laser2 = 11;
const int pRes1 = A0;
const int pRes2 = A1;
void setup() {
	Serial.begin(115200);
	pinMode(LED_BUILTIN, OUTPUT);
	pinMode(laser1, OUTPUT); //output for first laser
	pinMode(laser2, OUTPUT); //output for second laser
	pinMode(pRes1, INPUT); //input pin for photoresistor 1
	pinMode(pRes2, INPUT); //input pin for photoresistor 2
}
void loop() {
	digitalWrite(laser1, HIGH); //laser is on
	digitalWrite(laser2, HIGH); //laser is on
	Serial.print("Photoresistor Readings = ");
	value1 = analogRead(pRes1);
	value2 = analogRead(pRes2);
	delay(20);
	if(value1 > 1000 && value2 > 1000)//if signal gives a value above 950, i.e. if laser is
hitting the p.resistor
	{
		digitalWrite(LED_BUILTIN, HIGH);
		Serial.print(value1);
		Serial.print('\t');
		Serial.println(value2);
	}
	else if (value1 > 1000 && value2 < 1000)
	{
		digitalWrite(LED_BUILTIN, LOW);
		Serial.print(value1);
		Serial.print('\t');
		Serial.print(value2);
		Serial.print('\t');
		Serial.println(" <-- Laser 2 Blocked!");
	}
	else if (value1 < 1000 && value2 > 1000)
	{
		digitalWrite(LED_BUILTIN, LOW);
		Serial.print(value1);
		Serial.print('\t');
		Serial.print(value2);
		Serial.print('\t');
```

```
            Serial.println(" <-- Laser 1 Blocked!");
        }
        else if (value1 < 1000 && value2 < 1000)
        {
            digitalWrite(LED_BUILTIN, LOW);
            Serial.print(value1);
            Serial.print('\t');
            Serial.print(value2);
            Serial.print('\t');
            Serial.println(" <-- Both Lasers Blocked!");
        }
}
```

Appendix II: Calculation of Angles for Alignment of Laser Diodes

A little consideration shows that by symmetry, the angles of holes equidistant from the center will be equal to each other.

Snell's Law of Refraction, for light passing from air to a medium of refractive index μ:

$$\frac{\sin i}{\sin r} = \mu$$

Through measurement, we find the refracted angles.

For a 6-laser layer:

Outermost laser:

Angle of refraction = 29.48°

∴ Angle of incidence $i = \sin^{-1}(\mu \sin r)$

$i = \sin^{-1}(1.33 \times \sin 29.48)$

$i = 40.88°$

Middle-outer laser:

Angle of refraction = 17.17°

∴ Angle of incidence $i = \sin^{-1}(\mu \sin r)$

$i = \sin^{-1}(1.33 \times \sin 17.17)$

$i = 23.12°$

Inner laser:

Angle of refraction = 5.65°

∴ Angle of incidence $i = \sin^{-1}(\mu \sin r)$

$i = \sin^{-1}(1.33 \times \sin 5.65)$

$i = 7.52°$

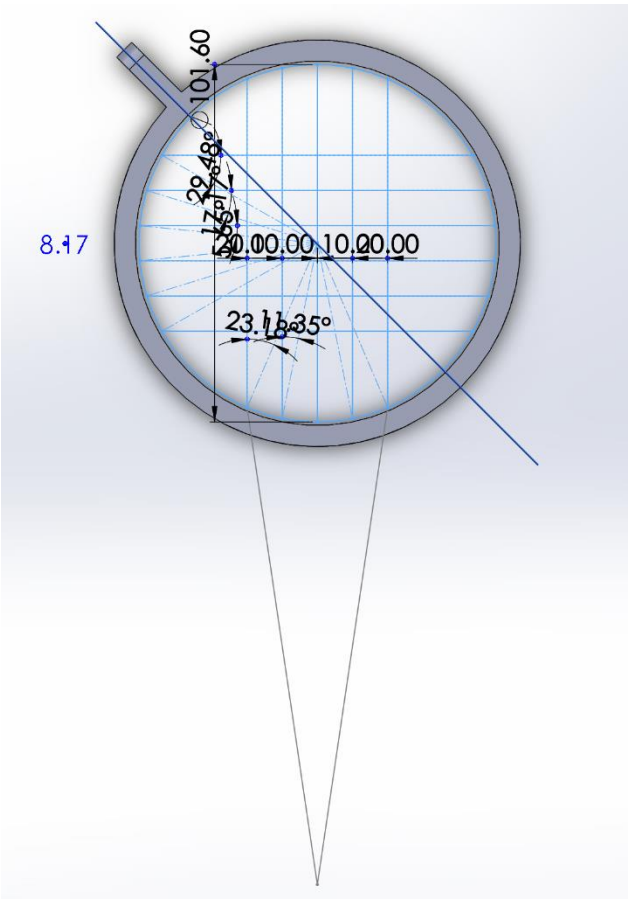

Figure 6.1: Calculations of Angles of Orientation for Laser Diodes

For a 5-laser layer:

Outermost laser:

Angle of refraction = 23.18°

∴ Angle of incidence $i = \sin^{-1}(\mu \sin r)$

$$i = \sin^{-1}(1.33 \times \sin 23.18)$$

$$i = 31.58°$$

Middle laser:

Angle of refraction = 11.35°

∴ Angle of incidence $i = \sin^{-1}(\mu \sin r)$

$$i = \sin^{-1}(1.33 \times \sin 29.48)$$

$$i = 15.18°$$

Inner (central) laser:

Since hole is radially opposite,

∴ angle of incidence = angle of refraction = 0°

References

[1] S. P. Evgenidis and T. D. Karapantsios, "Gas–liquid flow of sub-millimeter bubbles at low void fractions: Experimental study of bubble size distribution and void fraction," *International Journal of Heat and Fluid Flow,* 2018, pp. 353-365.

[2] A. Dragomirescu, I. Pincovschi and M. Miu, "Assessment of Global Void Fraction in a Gas-Liquid Stirred Vessel by Digital Image Processing," *Energy Procedia,* no. 112, 2017, pp. 217-224.

[3] J. A. Milkie, S. Garimella and M. P. Macdonald, "Flow regimes and void fractions during condensation of hydrocarbons in horizontal smooth tubes," *International Journal of Heat and Mass Transfer,* vol. 92, no. 1, 2016, pp. 252-267.

[4] M. Fukuta et al., "Quality Measurement of Two Phase Flow with Plug Flow," in *17th International Refrigeration and Air Conditioning Conference at Purdue*, 2018.

[5] H. Li et al., "A New Void Fraction Measurement Method for Gas-Liquid Two-Phase Flow in Small Channels," *Sensors,* no. 16, 2016, pp. 159-172.

[6] K. Sarkodie, A. Fergusson-Rees and P. Diaz, "A review of the application of non-intrusive infrared sensing for gas–liquid flow characterization," *The Journal of Computational Multiphase Flows,* vol. 10, no. 1, 2018, pp. 43-56.

[7] C. Wang et al., "Void Fraction Measurement Using NIR Technology for Horizontal Wet-Gas Annular Flow," *Experimental Thermal and Fluid Science,* no. 76, 2016, pp. 98-108.

[8] J. A. Malmstrom, K. F. Beck and S. D. Miles, "Optical Bubble Detection System". United States of America Patent 6,750,468 B2, 15 June 2004.

[9] M. J. Da Silva et al., "Experimental Investigation of Horizontal Gas-Liquid Slug Flow by Means of Wire-Mesh Sensor," *Journal of the Brazilian Society of Mechanical Sciences and Engineering ,* vol. SPE1, no. 33, 2010, pp. 234-242.